Power-law Fluid Velocity Profiles in Turbulent Pipe Flow

Chapter · January 1986

CITATIONS
4

READS
399

1 author:

Aroon Shenoy
SAICO
174 PUBLICATIONS **3,620** CITATIONS

SEE PROFILE

CHAPTER 31

POWER-LAW FLUID VELOCITY PROFILES IN TURBULENT PIPE FLOWS

A. V. Shenoy

Chemical Engineering Division
National Chemical Laboratory, India

CONTENTS

INTRODUCTION

Turbulent flow in non-Newtonian fluids has received much less attention than Newtonian fluids because it was believed that conditions of turbulence would theoretically never be reached in the case of non-Newtonian fluids due to their high consistencies. This was, however, later realized to be false and it is now generally accepted that turbulent flow of non-Newtonian fluids is not uncommon. The complexities of the rheological characteristics of the non-Newtonian fluids coupled with the chaotic random motions of the fluid particles when under turbulent conditions make the fluid mechanics rather difficult to handle theoretically. Hence, the approach to understanding turbulence in non-Newtonian fluids has been largely restricted to empirical correlations based on accumulated results of experimental observations of the time-averaged velocity profile and the pressure gradient, both of which are highly sensitive parameters.

This chapter deals with the velocity profiles in turbulent pipe flows of inelastic non-Newtonian fluids. It is restricted to only one type of fluid model to describe the rheological characteristics of the fluid, namely, the power-law model, as it is the simplest in form and yet describes the nature of several non-Newtonian fluids of industrial importance. In the case of turbulent flow of inelastic non-Newtonian fluids, this is the only model that has been used mainly because the added complexities of the other models lead to highly intricate mathematics. This chapter is limited to the fluid type but not to the flow situation, and considers turbulent flows through different geometrical pipe

cross-sections, through annular ducts, and even curved tubes. Power-law fluid velocity profiles are considered in all cases for smooth internal surfaces. Only in the case of the straight tubes are the velocity profile changes due to the effect of roughness of the pipe considered. In all cases, the fully developed velocity profiles are studied but an approach to estimate the hydrodynamic entrance lengths in the case of power-law fluids is given.

FLUID MODEL

It is well known that liquids with complex structure, such as macromolecular fluids, soap solutions, and two-phase fluid systems, do not follow the usual simple Newtonian relationship between the shear stress and shear rate. In fact, the proportionality parameter relating shear stress and shear rate is not a constant for complex fluids but varies with shear-rate. The shear-rate dependency of this parameter, which is nothing but the viscosity of the system, is a very important property of the fluid to be considered during flow situations. Depending on whether the viscosity increases or decreases with shear rate, we have a dilatant (shear-thickening) fluid or pseudoplastic (shear-thinning) fluid. A typical rheogram for a shear-thinning fluid is shown in Figure 1. Note that the constant viscosity behavior of a Newtonian fluid is only shown for comparison. Most non-Newtonian fluids behave as Newtonian fluids in the two limiting cases of very low shear rates and very high shear rates. The Newtonian viscosities in these two limits, namely, η_0 and η_∞, are of course quite different in value and often by orders of magnitude. The very low shear rate limiting viscosity would be of importance during laminar flow conditions; however, it is quite unlikely that the very high shear rate viscosity η_∞ would be reached even under normal turbulent conditions. The dashed line in Figure 1 shows the portion of the rheogram where the viscosity varies linearly with shear rate on the log-log plot. This tilted straight line can be described by a power-law expression of the following

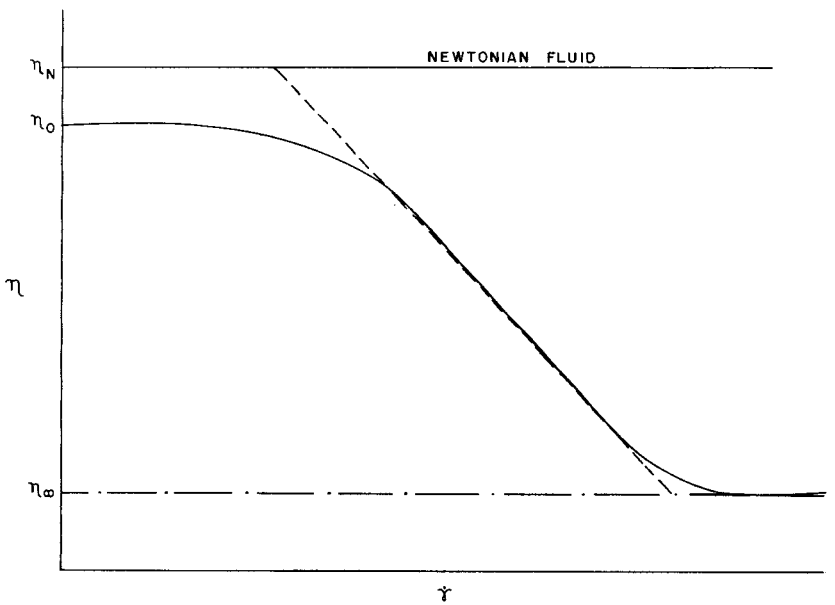

Figure 1. A typical viscosity versus shear rate curve for a pseudoplastic fluid on a double logarithmic plot. The constant Newtonian viscosity of a typical simple fluid is shown for comparison.

form:

$$\eta = K\dot{\gamma}^{n-1} \tag{1}$$

In Equation 1, K is often termed as the consistency index and n the power-law index. It is this linear portion of the viscosity versus shear rate curve described by Equation 1 that has assumed the most importance in the case of non-Newtonian fluid flow under turbulent conditions. The relationship between shear stress and shear rate for such fluids, whose rheogram is represented by Equation 1 in the linear portion is given by

$$\tau = K\dot{\gamma}^{n} \tag{2}$$

Equation 2 is conventionally known as the Ostwald-de Waele or power-law representation of the non-Newtonian fluids. Many polymer solutions or melts, biological fluids, suspensions, etc. can be described by this model. There are many useful models for describing the non-Newtonian characteristics of inelastic fluids [1], but the Ostwald-de Waele model is the most well known and widely used empiricism in many engineering problems. The flow model works excellently in all steady-state situations of pragmatic importance and describes the flow behavior of Newtonian ($n = 1$), shear-thinning ($n < 1$) and shear-thickening ($n > 1$) fluids. Values of n between 0.3 and 0.6 are quite common among most non-Newtonian fluids showing pseudoplastic behavior. It is possible to generate turbulence in pseudoplastic fluids but not in dilatant fluids because the increasing viscosity with shear rate in the latter case would dampen the turbulent motion.

VELOCITY PROFILES

The general methods for the development of expressions of power-law fluid velocity profiles and friction factors are on the same lines as those used in the case of Newtonian fluids, with of course the introduction of an additional degree of freedom by way of the flow behavior index n. Thus, in line with the traditional concepts that have been successfully used for Newtonian fluids, the turbulent flow of non-Newtonian fluids in smooth pipes, too, can be artificially divided into three zones as shown in Figure 2.

1. A laminar sublayer lying next to the pipe wall in which the effects of turbulence are negligible and whose thickness extending from the wall ($y = 0$) to $y = y_L$ is so thin that the shear stress across the layer can be assumed to be constant and equal to the wall shear stress.
2. A turbulent core comprising of the bulk of the fluid stream wherein the momentum transfer that accompanies the random velocity fluctuations characteristic of turbulent motion determines the velocity profile and the effects of viscosity are negligible.
3. A transition zone, between the laminar sublayer and the turbulent zone, in which the effects of turbulence and viscous shear are of comparable orders of magnitude.

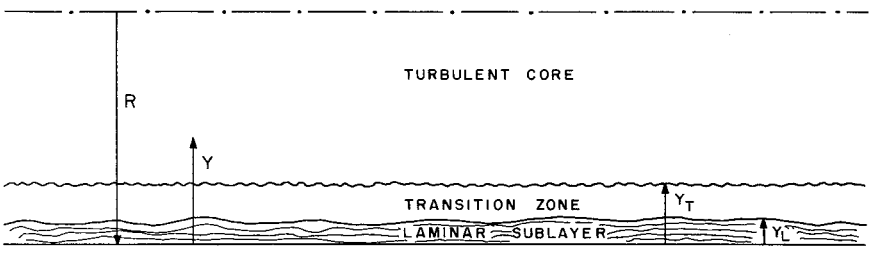

Figure 2. Schematic diagram of the highly idealized three-layer model for turbulent flow.

The thickness of the respective zones can be represented as follows:

Laminar sublayer: $0 < y < y_L$
Transition zone: $y_L < y < y_T$
Turbulent core: $y_T < y < R$

Smooth Straight Circular Pipes

For power-fluid turbulent flow in smooth straight circular pipes, the time-averaged velocity at a point would depend on six independent variables, namely, R, ρ, τ_w, K, n, y. Using conventional dimensional analysis as given by Langhaar [2], it can be shown that

$$\frac{u}{u^*} = \phi(R^+, y^*, n) \tag{3}$$

where u^* is the friction or shear velocity defined as $\sqrt{\tau_w/\rho}$, R^+ is the Reynolds number based on friction velocity defined as $R^n u^{*2-n}\rho/K$, and y^* is the dimensionless location parameter defined as y/R.

The theoretical development of the power-law fluid velocity profiles in turbulent flow through smooth straight circular pipes has been done by a number of investigators [3–6] and the typical nature of the predicted velocity profile is shown in Figure 3. The region of the transition is not well defined for power-law fluids. For Newtonian fluids, it has been established that the transition zone is given by $5 < y^+ < 30$, whereas the same is not the case for power-law fluids, and hence the point of change from the dashed line to the solid line in Figure 3 ought not to be taken seriously.

In each of the theoretical developments [3–6] there is unanimity in the expression for the velocity profile in the laminar sublayer. This is based on the highly idealized reasoning that there exists a viscous sublayer of thickness y_L in all turbulent flow situation where the velocity profile is linear and where the shear stress is constant and equal to the wall shear stress. For power-law fluids, the expression for the velocity profile in the viscous sublayer can be easily derived using Equation 2. Thus, for a velocity u at a distance y from the wall in the sublayer, we have

$$\tau_w = K\left(\frac{u}{y}\right)^n \tag{4}$$

Using the definition of friction velocity $u^* = \sqrt{\tau_w/\rho}$ as noted earlier, the expression for the velocity profile in the viscous sublayer can be written as

$$\frac{u}{u^*} = \left(\frac{\rho u^{*2-n} y^n}{K}\right)^{1/n} \tag{5}$$

or

$$u^+ = y^{+1/n} \quad \text{for} \quad y \le y_L \tag{6}$$

where u^+ is a dimensionless velocity and y^+ is distance based Reynolds number written in terms of the friction velocity, distance from the wall and fluid properties.

Dodge and Metzner [3] used a semi-theoretical analysis to derive the friction factor-Reynolds number relationship and the velocity profile in the turbulent core of a flowing purely viscous non-Newtonian fluid of the power-law type. Their expression for the velocity profile in the turbulent core is as follows:

$$u^+ = \frac{5.66}{n^{0.75}} \log y^+ \frac{-0.40}{n^{1.2}} + \frac{2.458}{n^{0.75}}\left[1.960 + 1.255n - 1.628n \log\left(3 + \frac{1}{n}\right)\right] \tag{7}$$

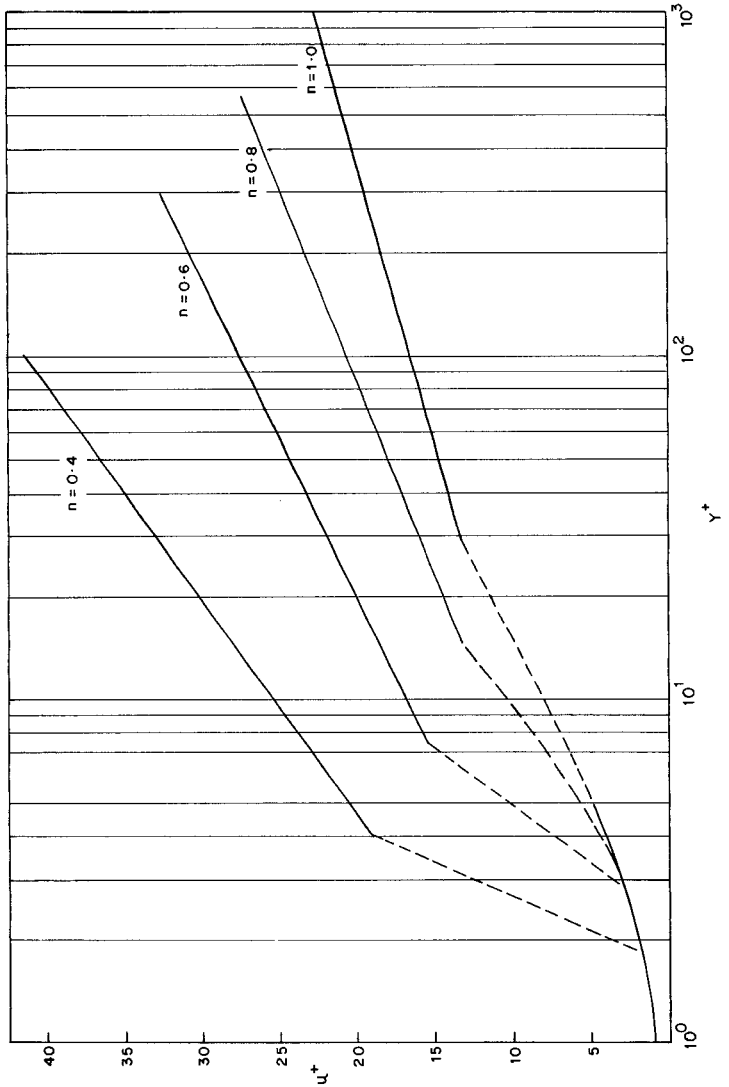

Figure 3. The typical shape of the velocity profile in the three-layer model for turbulent flow of power-law fluids.

An improvement in this expression was suggested by Bogue and Metzner [4], and a new expression of the following form was suggested for the velocity profile in the turbulent core:

$$u^+ = 5.57 \log y^{+1/n} + C(y^*, f) + I(n, Re_{gen}) \tag{8}$$

where $C(y^*, f)$ is a correction function defined as

$$C(y^*, f) = 0.05 \sqrt{\frac{2}{f}} \exp \frac{-(y^* - 0.8)^2}{0.15} \tag{9}$$

with the expression for friction factor for power-law fluids given as

$$\frac{1}{\sqrt{f}} = \frac{4.0}{n^{0.75}} \log Re_{gen} f^{(2-n)/2} - \frac{0.4}{n^{1.2}} \tag{10}$$

The values of the function $I(n, Re_{gen})$ are tabulated in Table 1 as taken from Bogue and Metzner [4].

The expressions proposed by Dodge and Metzner [3] and Bogue and Metzner [4] presume a two-layer rather than the three-layer model. They have not explicitly provided an expression for the buffer layer (transition zone). Clapp [5], however, has followed the three-layer model and provided expressions for the velocity profile for power-law fluids in turbulent flow by using the Prandtl and von Karman approach for Newtonian fluids. The three expressions for the universal velocity profile as obtained by Clapp [5] are:

Laminar sublayer—

$$u^+ = y^{+1/n} \qquad (0 \le y^+ \le 5^n) \tag{11}$$

Buffer layer—

$$u^+ = 5.0 \ln y^{+1/n} - 3.05 \qquad (5^n \le y + \le y_2^+) \tag{12}$$

Turbulent core—

$$u^+ = 2.78 \ln y^{+1/n} + \frac{3.8}{n} \qquad (y^+ > y_2^+) \tag{13}$$

The logarithmic expressions for the velocity profile in the turbulent core as given by Equations 7, 8, and 13 have an advantage to predict the velocity distributions beyond the range of experimentation due to their asymptotic nature. But each of the three expressions for the turbulent core have an incongruity implicitly hidden within them, namely that they fail to predict a zero velocity

Table 1
Values of the Function $I(n, Re_{gen})$ [4]

	Re_{gen}			
n	**5,000**	**10,000**	**50,000**	**100,000**
1.0	5.57	5.57	5.57	5.57
0.8	6.01	5.92	5.69	5.58
0.6	6.78	5.51	5.89	5.60
0.4	8.39	7.70	6.27	5.60

gradient at the center. However, the new velocity profile model as suggested by Shenoy and Saini [6] is devoid of this limitation and is, therefore, the correct theoretical velocity profile expression for turbulent core in the case of power-law fluids.

Shenoy and Saini [6] assumed a similar form of expression for the velocity profile as that of Bogue and Metzner [4], such that

$$u^+ = A(n)[\ln y^{+1/n} + C(y^*, n)] + B(n) \tag{14}$$

The correction function C(y*, n), however, was assumed to be of a different form unlike the one used earlier [4] as given by Equation 9. The following form was chosen:

$$C(y^*, n) = \sigma_1(n) \exp\left\{-\frac{1}{2}\left[\frac{y^* - 0.8}{\sigma_2(n)}\right]^2\right\} \tag{15}$$

This form for the correction function had two distinct advantages. Firstly, they could determine the expressions for $\sigma_1(n)$ and $\sigma_2(n)$ with a precondition such that it would allow the velocity gradient to go to zero at the centerline and secondly, because Equation 15 is independent of friction factor f, the correction function dependence is explicit on n as against the implicit dependence in earlier case of Equation 9.

Shenoy and Saini [6] derived the following expressions for $\sigma_1(n)$ and $\sigma_2(n)$:

$$\sigma_1(n) = 0.1944 - \frac{0.1313}{n} + \frac{0.3876}{n^2} - \frac{0.0109}{n^3} \tag{16}$$

$$\sigma_2(n) = \frac{0.254}{n} \tag{17}$$

From Equation 14, an implicit expression for friction factor can be easily derived and then compared with expression for friction factor of Dodge and Metzner [2] for power-law fluids as given by Equation 10 so that A(n) and B(n) can be determined. The final expression of Shenoy and Saini [6] for the velocity profile in the turbulent core is given as follows:

$$u^+ = 2.46n^{0.25}\left\{\ln y^{+1/n} + 0.1944 - \frac{0.1313}{n} + \frac{0.3876}{n^2} - \frac{0.0109}{n^3}\right.$$
$$\left.\exp\left[-\frac{n^2(y^* - 0.8)^2}{0.129}\right] + \frac{1.3676}{n} + \ln 2^{(2+n)/2n}\right\} - \frac{0.4\sqrt{2}}{n^{1-2}} \tag{18}$$

This velocity profile model was found to agree with the predictions of Bogue and Metzner [4] within a maximum deviation of $\pm 1.25\%$. It presently would thus stand as the most correct velocity profile for power-law fluids in the turbulent core based on its predictions and also its ability to attain a zero velocity gradient at the centerline for all values of n, which has been the main drawback in all earlier works.

The value of y* in the Equation 18 may be obtained by readjusting the terms in the definition of y^+. Thus

$$y^* = \left(\frac{y^+ 2^{(2+n)/2}}{Re_{gen} f^{(2-n)/2}}\right)^{1/n} \tag{19}$$

It is not always easy to get quick estimates of f required in the above expression without the use of an iterative procedure as can be seen from Equation 10. The following expression was, however, found to give values of f by direct substitution and simple calculations within an error bound of

$\pm 2.4\%$ for the entire range of n values between 1 and 0.3. Thus, the following equation may be used in preference to Equation 10, when friction factor values are to be estimated for power-law fluids for a range of generalized Reynolds number values between 4×10^3 and 10^6:

$$\frac{1}{\sqrt{f}} = 3.57 \log \frac{Re_{gen}^{n^{1/0.615}}}{6.5^{n^{1/(1+0.75n)}}} \tag{20}$$

where

$$Re_{gen} = \frac{D^n V^{2-n} \rho}{\gamma} \tag{21}$$

$$\gamma = K\left(\frac{1+3n}{4n}\right)^n 8^{n-1} \tag{22}$$

Though Equation 18 gives the correct description of the velocity profile for turbulent flow of power-law fluids, there is always a tendency to look for simpler expressions that could form a good engineering approximation to the exact one at least in a limited region. The one-seventh power-law expression for the velocity profile in the case of Newtonian fluids is an example of such an approach. The extension of the same for power-law fluids can be done very easily [7].

Dodge and Metzner [3] have provided the following Blasius type of approximate equation for friction factor $f = \phi(Re_{gen}, n)$ for turbulent flow of power-law fluids.

$$f = \frac{\alpha}{Re_{gen}^{\beta}} \qquad (5 \times 10^3 \leq Re_{gen} \leq 10^5) \tag{23}$$

The α and β values for varying n have been reported by them [3]. Noting that $\tau_w = (f/2)\rho V^2$, the following expression can be written using Equation 23:

$$\tau_w = \frac{\alpha}{2^{1+\beta n}} \rho V^{2-\beta(2-n)} \left(\frac{\gamma}{\rho}\right)^{\beta} R^{-\beta n} \tag{24}$$

By definition, $u^* = (\tau_w/\rho)^{1/2}$, and from Skelland [7] for turbulent flow of power-law fluids, V can be expressed in terms of the maximum velocity u_m:

$$V = \psi u_m \tag{25}$$

where

$$\psi = \frac{[2-\beta(2-n)][2-\beta(2-n)]}{[1-\beta(1-n)][4-\beta(4-3n)]} \tag{26}$$

Equation 24 can thus be transformed to give

$$\frac{u_m}{u^*} = \left[\frac{2^{1+\beta n}}{\alpha \psi^{2-\beta(2-n)}}\right]^{1/[2-\beta(2-n)]} \left[\frac{R^n u_m^{2-n} \rho}{\gamma}\right]^{\beta/[2-\beta(2-n)]} \tag{27}$$

The key assumption in order to get the simple velocity profile expression lies in an approximation that Equation 27 is valid at any wall distance y rather than only at R. Thus,

$$u^+ = A_1 y^{+B_1} \tag{28}$$

where

$$A_1 = \left[\frac{2^{1+\beta n}}{\alpha \psi^{2-\beta(2-n)}}\right]^{1/[2-\beta(2-n)]} \left[\left(\frac{4n}{1+3n}\right) 8^{1-n}\right]^{\beta/[2-\beta(2-n)]} \tag{29}$$

$$B_1 = \frac{\beta}{[2-\beta(2-n)]} \tag{30}$$

Equation 28 has several limitations. Its range of validity is limited to Reynolds number between 5×10^3 and 10^5. Further, it cannot predict a zero velocity gradient at the centerline; and due to the simplifying assumptions made in its derivation, it does not give an accurate description of the velocity profile. However, with all its shortcomings, it still would be a useful expression to be used in engineering design such as for calculating the turbulent entrance lengths for power-law fluids as will be shown later.

Arbitrary Cross-Sectional Pipes

Non-Newtonian flow through non-circular pipes has been studied in considerable detail by Kozicki et al. [8] and Salem and Embaby [9]. The work of Kozicki et al. [8] deals with laminar flow of incompressible time-independent non-Newtonian fluids in ducts of arbitrary cross-section, while Salem and Embaby [9] have dealt with laminar as well as turbulent flow conditions. However, there is no expression for turbulent velocity profile derived by them for power-law fluids. Salem and Embaby [9], nevertheless, have given an expression for the friction factor in non-circular pipes based on the equivalent pipe diameter as was used by Kozicki et al. [8] in their studies. Their suggested expression is as follows:

$$\frac{1}{\sqrt{f}} = \frac{4}{n^{0.75}} \log_{10}[Re^*_{gen} f^{(2-n)/2}] - \frac{0.4}{n^{1.2}} + 4.0n^{0.25} \log_{10}\left[\frac{4(a+bn)}{1+3n}\right] \tag{31}$$

where Re^*_{gen} is the generalized Reynolds number for power-law fluids in non-circular pipes based on the hydraulic radius r_H and defined as follows:

$$Re^*_{gen} = \frac{r_H^n V^{2-n} \rho}{2^{2n-3}\left[\frac{a+bn}{n}\right]^n K} \tag{32}$$

The form of Equation 31 is the same as Equation 10 for friction factor in smooth straight pipes, except for an extra term that incorporates the geometrical correction factor due to the non-circular nature of the pipe. A similar approach can be adopted to obtain an expression for the velocity profile in non-circular pipes of arbitrary cross-section. Equation 18 can be modified to include the geometrical parameters for the cross-sectional shape and thus the following equation can be written:

$$u^+ = 2.46n^{0.25}\left\{\ln y^{+1/n} + \left(0.1944 - \frac{0.1313}{n} + \frac{0.3876}{n^2} - \frac{0.0109}{n^3}\right) \exp\left[\frac{-n^2(y^* - 0.8)^2}{0.129}\right] + \frac{1.3676}{n} + \ln 2^{(2+n)/2n} + \ln\frac{4(a+bn)}{1+3n}\right\} - \frac{0.4\sqrt{2}}{n^{1.2}} \tag{33}$$

The definitions of u^+, y^+, y^* are the same as those in the smooth straight pipe case except for the difference in definition of the Reynolds number term (see Equation 32). The geometric parameters a and b for a wide variety of cross-sectional shapes of ducts have been determined by Kozicki

et al. [8] and their expressions as well as the values for certain specific cases have been well tabulated.

Equations 18 and 33 are identical but for the following term:

$$T = 2.46n^{0.25} \ln \frac{4(a + bn)}{1 + 3n} \tag{34}$$

This term controls the change in the shape of the velocity profile depending on the geometry of the conduit. Hence, it is worth looking at the variations of the term T for different geometrical shapes and different values of n. The values of T for a wide variety of specific cases are evaluated and tabulated in Table 2. The cases include various types of cross-sectional geometries such as elliptical, rectangular, and isosceles triangular ducts for typical values of a and b taken from Kozicki et al. [8]. The parametric space covered, thus, includes a number of power-law fluid types flowing through ducts of different shapes and sizes. It should be noted that the term T would be identically equal to zero for all values of power-law index for a circular pipe. It can be seen from Table 2 that T takes values between -0.55 and $+0.33$ in all cases and hence does not form an important term in Equation 33. Thus, the velocity profile in effect could be predicted by Equation 18 given earlier for smooth straight circular pipes. This, however, does not imply that the velocity profiles are the same for all cross-sectional shapes. It must be noted that the dimensionless parameter now includes a modified Reynolds number based on the hydraulic radius factor, which would be different for various geometrical shapes. Thus, though the dimensionless velocity profiles are predicted as identical by Equation 33, the actual variation in the velocity shape does exist. There is presently no experimental work in the literature to substantiate these findings.

Annular Pipes

Flow of non-Newtonian fluids in annuli has been comprehensively studied by Tan and Tiu [10–13] and Bhattacharyya and Tiu [14 and 15]. However, they deal with only the laminar case and as far as turbulent flow of non-Newtonian fluids is concerned, there is a complete lack of information in the literature. Nevertheless, the fully developed turbulent velocity profile for flow of an inelastic non-Newtonian fluid can be easily derived based on the simple power-law type expression given by Equation 28 for smooth circular pipe.

In flow through an annulus, the flow model ought to be divided into two regions, namely, the outer region and the inner region as a consequence of the two wall boundaries. Each region would therefore have a separate velocity profile. It is now assumed that the effect of the inner cylinder on the velocity profile in the outer region is small enough to be neglected. It can thus be treated in a manner analogous to a smooth straight pipe so that Equation 28 would hold reasonably well. Thus,

$$u_o^+ = A_1 y_o^{+B_1} \tag{35}$$

where the subscript o represents the outer region of the annulus and A_1 and B_1 have the same forms as given by Equations 29 and 30, respectively.

It is now assumed that an expression of the similar form as Equation 35 would hold for the inner region as

$$u_i^+ = \bar{A}_1 y_i^{+B_1} \tag{36}$$

where the subscript i represents the inner region of the annulus, and $\bar{A}_1$ and $\bar{B}_1$ are to be determined for this region. In order to obtain expressions for $\bar{A}_1$ and $\bar{B}_1$, we would have to go through complicated mathematical procedures leading to expressions that would be too cumbersome for

Table 2
Values of T Given by Equation 34, for Different Non-Circular Pipe Shapes at Typical Values of n

Pipe shape	a	b	n	T
Elliptical $\frac{b'}{a'} = 0.3$	0.2796	0.8389	1.0	0.2645
			0.8	0.2507
			0.6	0.2341
			0.4	0.2127
$\frac{b'}{a'} = 0.5$	0.2629	0.7886	1.0	0.1235
			0.8	0.1168
			0.6	0.1088
			0.4	0.0983
$\frac{b'}{a'} = 0.7$	0.2538	0.7614	1.0	0.0371
			0.8	0.0351
			0.6	0.0327
			0.4	0.0295
Rectangular $\frac{b'}{a'} = 0.25$	0.3212	0.8182	1.0	0.3209
			0.8	0.3211
			0.6	0.3217
			0.4	0.3222
$\frac{b'}{a'} = 0.50$	0.2440	0.7276	1.0	−0.0709
			0.8	−0.0664
			0.6	−0.0610
			0.4	−0.0540
$\frac{b'}{a'} = 0.75$	0.2178	0.6866	1.0	−0.2472
			0.8	−0.2388
			0.6	−0.2289
			0.4	−0.2163
Isoceles $2\alpha' = 20°$ Triangular Duct	0.1693	0.6332	1.0	−0.5413
			0.8	−0.5334
			0.6	−0.5252
			0.4	−0.5156
$2\alpha' = 40°$	0.1840	0.6422	1.0	−0.4697
			0.8	−0.4592
			0.6	−0.4474
			0.4	−0.4326
$2\alpha' = 60°$	0.1875	0.6462	1.0	−0.4474
			0.8	−0.4369
			0.6	−0.4251
			0.4	−0.4101

engineering applications. The situation, however, becomes greatly simplified if it is assumed that the slopes of the u_o^+ versus y_o^+ and the u_i^+ versus y_i^+ are the same, thus giving $\bar{B}_1 = B_1$.

The momentum balance for the inner and outer flow region of the annuli gives the following expressions for wall shear stresses τ_{wi} and τ_{wo}:

$$\tau_{w_i} = \frac{r_i}{2}\left[\frac{\lambda^2}{k^2} - 1\right]\frac{\Delta P}{L} \tag{37}$$

$$\tau_{w_o} = \frac{r_o}{2}[1 - \lambda^2]\frac{\Delta P}{L} \tag{38}$$

where

$$\lambda = \frac{r_m}{r_o}, \qquad k = \frac{r_i}{r_o} \tag{39}$$

In these equations, r_i, r_o, and r_m represent the radius of the inner cylinder, radius of the outer pipe and radius of maximum velocity, respectively.

Using the definition of $u^* = \sqrt{\tau_w/\rho}$ for the inner and outer region, the following expression can be easily derived. Thus,

$$\frac{u_o^*}{u_i^*} = \left[\frac{k(1-\lambda^2)}{(\lambda^2 - k^2)}\right]^{1/2} \tag{40}$$

Using the fact that $u_i = u_o$ at $r = r_m$, the expression for $\bar{A}_1$ can be obtained as

$$\bar{A}_1 = A_1\left[\frac{k(1-\lambda^2)}{(\lambda^2 - k^2)}\right]^{B'}\left[\frac{1-\lambda}{\lambda - k}\right]^{B_1 n} \tag{41}$$

where

$$B' = \frac{(2-n)B_1 + 1}{2} \tag{42}$$

Thus, the velocity profile for the inner region of the annulus can be written in the following form:

$$u_i^+ = A_1\left[\frac{k(1-\lambda^2)}{(\lambda^2 - k^2)}\right]^{B'}\left[\frac{1-\lambda}{\lambda - k}\right]^{B_1 n} y_i^{+B_1} \tag{43}$$

Equations 35 and 43 thus define the complete velocity profile for power-law fluids in an annulus. There is no experimental data in the literature to support these theoretical predictions but the expressions just given would provide the guidelines for the expected trend.

Curved Pipes

The study of transport processes in curved pipes is of considerable pragmatic importance because of the significant advantages that such a configuration offers when used for heat/mass transfer purposes or as chemical reactors. From a fluid mechanics point of view, curved pipes represent an interesting flow situation due to the effects of curvature. A secondary flow is set up by virtue of the centrifugal force that gets superimposed on the axial velocity flow field. The central fluid is actually driven towards the outer wall and is then pushed back along the wall towards the inner

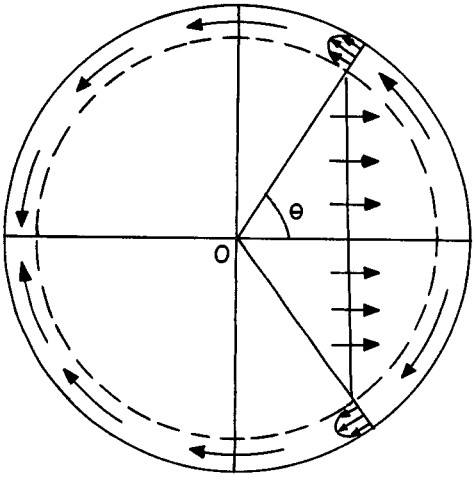

Figure 4. Schematic representation of the flow model for curved pipes showing the boundary layer, the inviscous core and the continuity of secondary flow. (From Mashelkar and Devarajan [16].)

side. A double vertical motion is thus set up and a flow situation of the kind shown schematically in Figure 4 results.

The only work on turbulent flow of power-law fluids in curved pipes available in the literature is that of Mashelkar and Devarajan [16]. Their theoretical approach considers the flow to be representable by a two region model—a central inviscous core and a thin boundary layer near the wall as shown in Figure 4. The momentum integral equations for the turbulent boundary layer flow were solved numerically by them to obtain the velocity distribution in the curved pipe. Mashelkar and Devarajan [16] assumed the following forms for the angular and axial velocity distributions in the boundary layer:

$$V = D_1\left(\frac{\xi}{\delta}\right)^{\beta n/[2-\beta(2-n)]}\left(1-\frac{\xi}{\delta}\right) \tag{44}$$

$$w = w_1\left(\frac{\xi}{\delta}\right)^{\beta n[2-\beta(2-n)]} \tag{45}$$

where $\zeta = \bar{a} - r$ with $\bar{a}$ as the radius of the pipe and r the radial position. δ is the boundary layer thickness.

Using the following expressions:

$$\delta = \delta_c \bar{a}\{[Re(\bar{a}/\bar{R})^{1/2\beta}\}^{-\beta/(\beta n+1)} \tag{46}$$

$$D_1 = D_c(v_m\sqrt{\bar{a}/\bar{R}}) \tag{47}$$

$$w_1 = w_c(v_m) \tag{48}$$

the differential equations are non-dimensionalized and the values of δ_c, D_c, and w_c are obtained by expanding in the neighborhood of $\theta = o$ using

$$\delta_c = \delta_1(1 + \delta_2\theta^2 + \cdots) \tag{49}$$

$$D_c = D_2\theta(1 + D_3\theta^3 + \cdots) \tag{50}$$

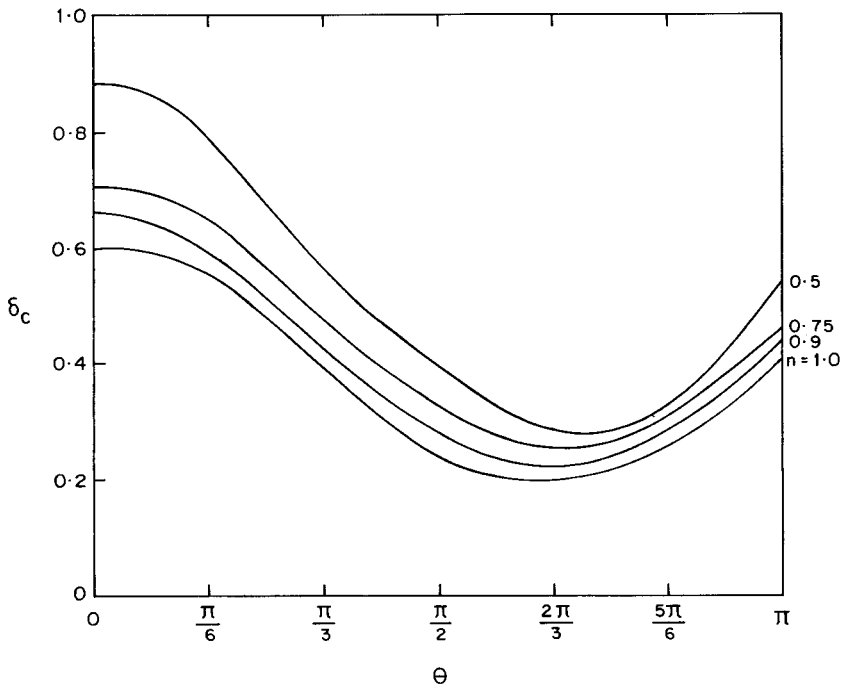

Figure 5. Variation of dimensionless turbulent boundary layer δ_0 with θ for varying pseudoplasticity index n. (From Mashelkar and Devarajan [16].)

and

$$w_c = 1 + \frac{\bar{B}\bar{a}}{V_m}\left(1 - \frac{\theta^2}{2!} + \frac{\theta^4}{4!} - \cdots\right) \tag{51}$$

In these equations $\bar{R}$ is the radius of curvature of the pipe, v_m is the mean axial velocity, and θ is the angular position in cylindrical co-ordinates. Using a Runge-Kutta-Merson technique, the integration of the differential equations yields the variation of the non-dimensionalized turbulent boundary layer thickness, δ_0, the non-dimensionalized axial velocity w_c at the outer edge of the boundary layer and the non-dimensionalized characteristic angular velocity D_c with θ. Figures 5–7 show the functions $\delta_c(\theta)$, $w_c(\theta)$, and $D_c(\theta)$ for power-law fluids with different pseudoplasticity indices. It can be seen that the dimensionless angular velocity decreases with increasing pseudoplasticity over the entire range of θ whereas the dimensionless axial velocity decreases with increasing n for $0 < \theta < \pi/2$ but increases with increasing n for $\pi/2 < \theta < \pi$ indicating the change in the steepness of the velocity profile for increasing pseudoplasticity. The information available from these figures along with Equations 44–48 describes the velocity profiles in the boundary layer during the turbulent flow of power-law fluids through curved pipes. The velocity distribution in the central core is given by the following expression through a straightforward derivation from the equation of motion:

$$w = v_m\left[1 + \left(\frac{\bar{B}\bar{a}}{v_m}\right)\frac{r}{\bar{a}}\cos\theta\right] \tag{52}$$

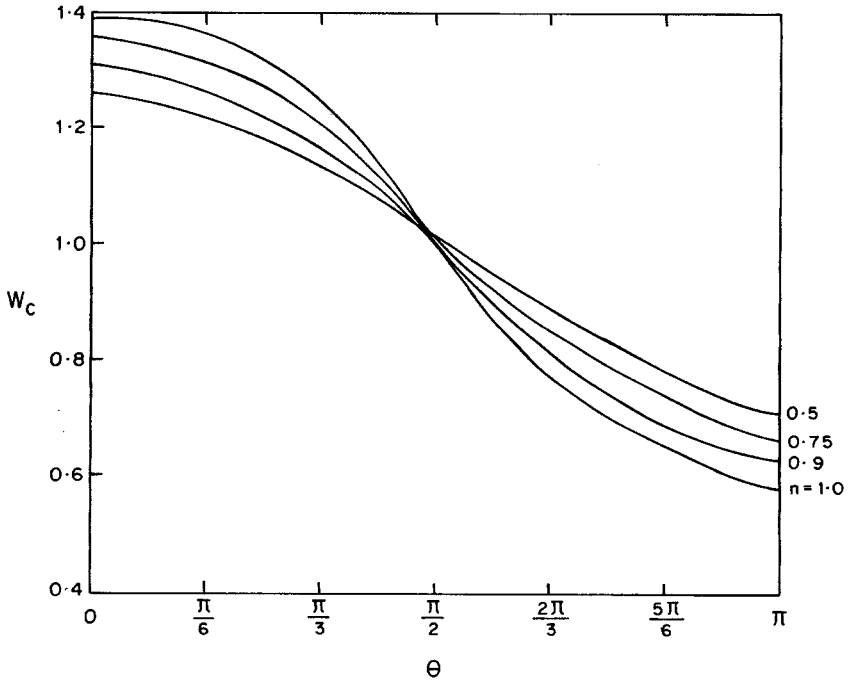

Figure 6. Variation of dimensionless axial velocity at the outer edge of the boundary layer w_0 with θ for varying pseudoplasticity index n. (From Mashelkar and Devarajan [16].)

The values of $\bar{B}\bar{a}/v_m$ for varying pseudoplasticity index are given in Table 3. The entire velocity distribution for turbulent flow of power-law fluids through curved pipes is thus made available. Mashelkar andd Devarajan [16] have provided experimental data on only friction factor and have not made any velocity profile measurements for verification of their theoretical predictions.

Rough Pipes

The developments of all the velocity profiles in the foregoing sections were based on the assumption that the inside wall of the pipe surface is smooth and free from defects. This, of course, is an idealized situation as in practice all pipes have a certain degree of roughness even when they are new. Those that have been in service for a while, invariably develop some surface defects. In order to give a complete description of the roughness, one would have to give detailed dimensions of the protrusions or indentations, which is impractical. However, it is understandable that the actual dimensions of the roughness should not have as great an effect as the relative roughness due to the size of the protrusions or indentations in comparison to the dimensions of the pipe. Figure 8 shows a schematic diagram of the roughness of a surface. The average height of the roughness projections is expressed as ϵ and thus the relative roughness of the tube is written by the factor ϵ/D. This would mean that for smooth tubes, the relative roughness factor is zero.

For laminar flow, there is no influence of the relative roughness on the velocity distribution. However, for turbulent flow, the nature of the flow is intimately related to surface roughness. The roughness will be effective as long as the laminar sublayer near the wall is thin compared to the ϵ/D and this would happen at increased Reynolds numbers. Thus, a rough surface does not always

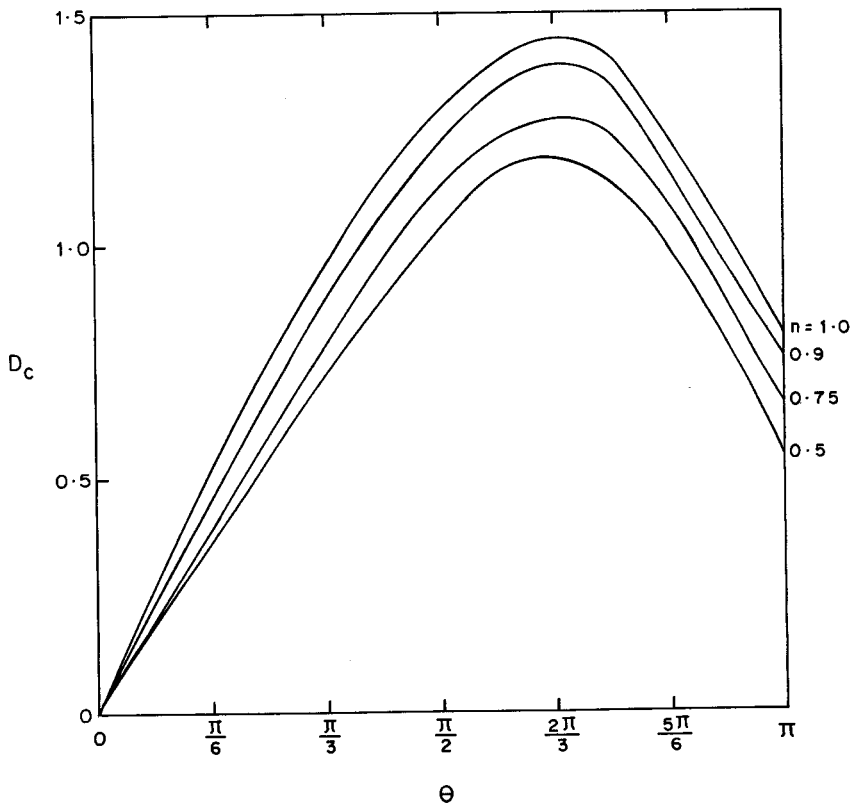

Figure 7. Variation of dimensionless characteristic angular velocity D_0 with θ for varying pseudoplasticity index n. (From Mashelkar and Devarajan [16].)

act rough but depends on the relative magnitude of the size of the surface roughness elements and the thickness of the viscous sublayer. A roughness Reynolds number may be defined for power-law fluids by substituting in the expression for y^+ given in Equation 5 the value of $y = \epsilon$ to give

$$Re_\epsilon = \frac{\rho u^{*2-n}\epsilon^n}{K} \tag{53}$$

Table 3
Values of $\bar{B}\bar{a}/V_m$ for Varying Pseudoplasticity Index [16]

n	$\frac{\bar{B}\bar{a}}{V_m}$
1.0	0.37803
0.9	0.36988
0.75	0.31824
0.5	0.26894

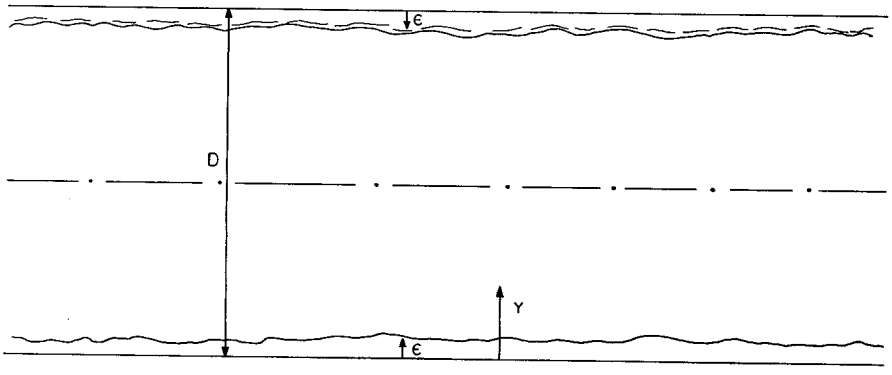

Figure 8. Schematic diagram of the roughness of a pipe surface.

or

$$Re_\epsilon = \left(\frac{\epsilon}{D}\right)^n Re_{gen}\left(\frac{f}{2}\right)^{(2-n)/2} \tag{54}$$

For power-law fluids, as long as the value of $Re_\epsilon < 5^n$ the roughness would be covered by the laminar sublayer and then the resulting flow would take place as if in the smooth pipe. However, for $Re_\epsilon > 5^n$ the roughness of the pipe would affect both the friction factor and the velocity profile. The expression for the velocity profile for power-law fluids under fully rough wall turbulence has been provided by Torrance [17] as

$$u^+ = 2.5 \ln\left(\frac{y}{\epsilon}\right)^{1/n} + 8.5 \tag{55}$$

Equation 55 again suffers from the limitation of not being able to predict the velocity gradient as zero at the centerline. A new expression similar to Equation 18 could certainly be derived by making some reasonable assumptions.

A modified form of Equation 18 can be written as

$$u^+ = 2.46n^{0.25}\left\{\ln\left(\frac{y}{\epsilon}\right) + \ln\left(\frac{\rho u^{*2-n}\epsilon^n}{K}\right)^{1/n} + \left(0.1944 - \frac{0.1313}{n} + \frac{0.3876}{n^2} - \frac{0.0109}{n^3}\right) \times \exp\left[-\frac{n^2(y^* - 0.8)}{0.129}\right] + \frac{1.3676}{n} + \ln 2^{(2+n)/2n}\right\} - \frac{0.4\sqrt{2}}{n^{1.2}} \tag{56}$$

The only extra term that comes in due to the roughness of the pipe is the term T_1 as defined below, which needs to be evaluated:

$$T_1 = 2.46n^{0.25} \ln\left(\frac{\rho u^{*2-n}\epsilon^n}{K}\right)^{1/n} \tag{57}$$

For the evaluation of this term we consider the velocity profile expression for Newtonian fluid for smooth and rough pipes and find the difference. Thus,

For smooth pipes—

$$u^+ = 2.5 \ln y^+ + 5.5 \tag{58}$$

For rough pipes—

$$u^+ = 2.5 \ln\left(\frac{y}{\epsilon}\right) + 8.5 \tag{59}$$

It can be concluded that the value of the term for Newtonian fluid is as follows:

$$2.5 \ln \frac{\rho u^* \epsilon}{K} = 3.0 \tag{60}$$

Thus,

$$\frac{\rho u^* \epsilon}{K} = 3.32 \tag{61}$$

The roughness Reynolds number is taken as 3.32 because, in fact, for Newtonian fluids [18] the roughness makes itself felt at $Re > 3$. In the case of non-Newtonian power-law fluids, we assume that the roughness would make itself felt at $Re > 3^n$. Thus, in an approximation we have

$$T_1 = 3.0n^{0.25} \tag{62}$$

Thus, the velocity profile for power-law fluids in rough pipes can be written as

$$u^+ = 2.46n^{0.25}\left\{\ln\frac{y}{\epsilon} + \left(0.1944 - \frac{0.1313}{n} + \frac{0.3876}{n^2} - \frac{0.0109}{n^3}\right)\exp\left[-\frac{n^2(y^* - 0.8)^2}{0.129}\right] + 1.2195 + \frac{1.3676}{n} + \ln 2^{(2+n)/2n}\right\} - \frac{0.4\sqrt{2}}{n^{1.2}} \tag{67}$$

A comparison between the predictions of Equations 55 and 63 shows reasonably close agreement.

ENTRANCE LENGTH ESTIMATION

Smooth Circular Pipes

The theoretical expressions for the velocity profiles given in foregoing sections of this chapter are all for the fully developed case. In order to get an idea of the fully developed region in any flow situation, one must have an estimate of the hydrodynamic entrance length. There is no information in the literature concerning turbulent entrance region flow of inelastic non-Newtonian fluids except for the work of Shenoy and Mashelkar [19] who have provided a method to get an engineering estimate of the hydrodynamic entrance lengths in non-Newtonian turbulent flow through smooth circular pipes. Their method involves an ordering technique to derive the turbulent hydrodynamic entrance lengths but they find that the predictions of their approximation approach give good agreement with existing data. They assumed that the simple velocity profile expression given by Equation 28 could be applied to the edge of the boundary layer (i.e. at $y = \delta$) where $u = u_o$, thus giving

$$\frac{u_o}{u^*} = \left[\frac{2^{1+\beta n}}{\alpha \psi^{2-\beta(2-n)}}\right]^{1/[2-\beta(2-n)]}\left[\frac{\delta^n u^{*2-n}\rho}{\gamma}\right]^{\beta/[2-\beta(2-n)]} \tag{64}$$

Rearranging Equation 64 and using $\tau_w = \rho u^{*2}$, gives the following

$$\tau_w = \frac{\alpha\psi^{2-\beta(2-n)}}{2^{1+\beta n}} \rho u_o^{2-\beta(2-n)} \left[\frac{\gamma}{\rho\delta^n}\right]^{\beta} \tag{65}$$

An alternative form for τ_w in the turbulent boundary layer has been provided by Skelland [7] as

$$\tau_w = \psi_1 \rho u_o^2 \frac{d\delta}{dx} \tag{66}$$

where

$$\psi_1 = \frac{[2-\beta(2-n)]}{[2-2\beta(1-n)]} - \frac{[2-\beta(2-n)]}{[2-\beta(2-3n)]} \tag{67}$$

Comparing Equations 65 and 66 and solving for δ gives

$$\delta = \left[\frac{(1+\beta n)}{\psi_1} \frac{\alpha\psi^{2-\beta(2-n)}}{2^{1+\beta n}}\right]^{1/(1+\beta n)} \left[\frac{\gamma}{\rho u_o^{2-n}}\right]^{\beta/(1+\beta n)} \left[\frac{1}{1+\beta n}\right] \tag{68}$$

In order to get an estimate of the turbulent entry length, x is set equal to x_e (the entrance length), δ is set equal to D/2 (the pipe centerline), and u_o is set equal to u_m (the maximum velocity at pipe centreline $= V/\psi$). Thus, by simplification the following expression for the turbulent entrance length for power-law fluids in smooth straight circular pipes is derived:

$$\frac{X_e}{D} = \left[\frac{\psi_1}{(1+\beta n)\alpha\psi^2}\right] Re_{gen}^{\beta} \tag{69}$$

Figure 9 shows a plot of the normalized dimensionless entrance lengths for turbulent flow through smooth straight circular pipes. The results indicate that increasing pseudoplasticity gives rise to larger entrance lengths. Dodge and Metzner [3] show that in a limited range $5 \times 10^3 < Re_{gen} < 10^4$, $0.6 < n < 1$, entrance length results for non-Newtonian fluids qualitatively agree with similar Newtonian measurements and are of a comparable magnitude or somewhat shorter. The results of Shenoy and Mashelkar [19] show a contrary trend and hence it might be erroneous to use Newtonian values for power-law fluids. In fact, making velocity measurements after an entrance length for Newtonian fluid could lead to errors as the flow is not fully developed until much greater lengths for pseudoplastic fluids. These findings would need experimental verification which are, unfortunately, not available in the existing literature.

Arbitrary Cross-Sectional Pipes

Presently, there is no clue whatsoever in the literature as to the magnitude of the turbulent entrance lengths in the case of power-law fluids flowing through conduits of various geometrical cross-sectional shapes. An exact solution of the hydrodynamic problem of turbulent non-Newtonian entrance region in non-circular pipes would, undoubtedly, be a more formidable task than in circular pipes. However, the design equation suggested by Shenoy and Mashelkar [19] for estimating the hydrodynamic turbulent entrance lengths for power-law fluids in circular pipes can be extended to include flow through conduits of arbitrary cross-sectional shape. Using an approach similar to that used earlier to obtain the velocity profile for arbitrary cross-sectional pipes, Equation 69 can be modified by appropriate manipulation of the terms to give

$$\frac{x_e}{2r_H} = \lambda_1 \left[\frac{\psi_1}{(1+\beta n)\alpha\psi^2}\right] Re_{gen}^{*\beta} \tag{70}$$

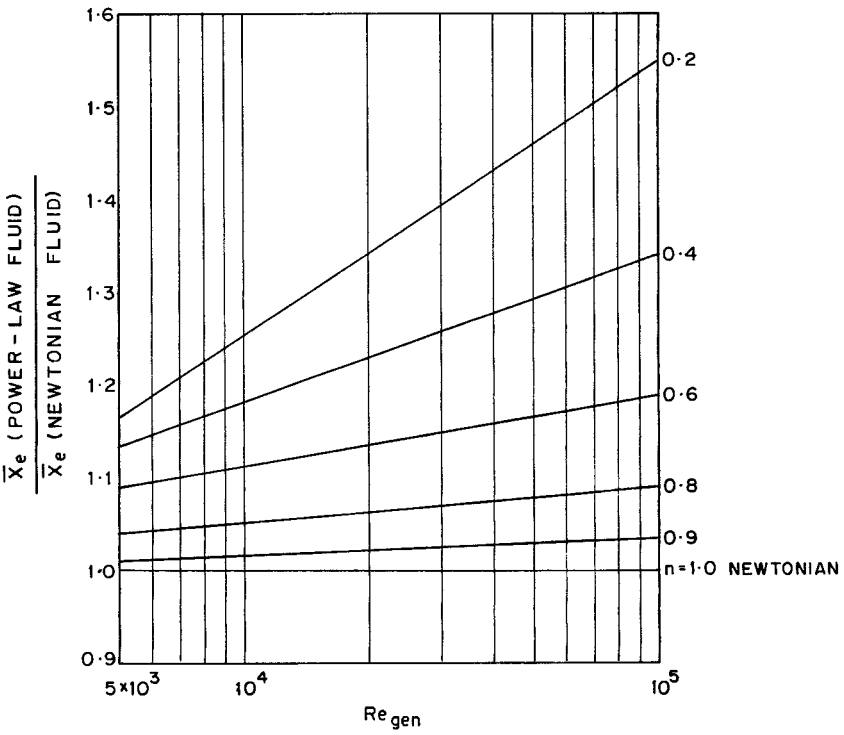

Figure 9. Estimated normalized turbulent entrance length ratios as a function of Reynolds number and the pseudoplasticity index n.

where

$$\lambda_1 = \left[\frac{4(a + bn)}{1 + 3n}\right]^{\beta n} \tag{71}$$

Defining the dimensionless entrance length $\bar{x}_c = x_e/D$ for circular pipes and $\bar{x}_{Nc} = x_e/2r_H$ for non-circular pipes, the following expression can be written when the Reynolds numbers in the circular and non-circular pipes are of the same magnitude. Thus,

$$\frac{\bar{x}_{Nc}}{\bar{x}_c} = \lambda_1 \tag{72}$$

The values of λ_1 for a wide variety of specific cases are evaluated and tabulated in Table 4. The cases include various types of cross-sectional geometries such as elliptical, rectangular, and isosceles triangular ducts for typical values of a and b taken from Kozicki et al. [8]. The values of λ_1 are seen to be not more than $\pm 5\%$ different from 1. Values of λ_1 less than one imply that the velocity profile develops earlier in these cases compared to the case of circular pipes. The fact that the values of λ_1 are not too different from one does not, however, imply that the entrance lengths

Table 4
Values of λ_1 Given by Equation 71 for Different Non-Circular Pipe Shapes at Typical Values

Pipe shape	a	b	n	β	λ_1
Elliptical $\frac{b'}{a'} = 0.3$	0.2796	0.8389	1.0	0.250	1.0284
			0.8	0.263	1.0238
			0.6	0.281	1.0191
			0.4	0.307	1.0138
$\frac{b'}{a'} = 0.5$	0.2629	0.7886	1.0	0.250	1.0126
			0.8	0.263	1.0106
			0.6	0.281	1.0085
			0.4	0.307	1.0062
$\frac{b'}{a'} = 0.7$	0.25338	0.7614	1.0	0.250	1.0038
			0.8	0.203	1.0032
			0.6	0.281	1.0025
			0.4	0.307	1.0019
Rectangular $\frac{b'}{a'} = 0.25$	0.3212	0.8182	1.0	0.250	1.0382
			0.8	0.263	1.0295
			0.6	0.281	1.0254
			0.4	0.307	1.0204
$\frac{b'}{a'} = 0.50$	0.2440	0.7276	1.0	0.250	0.9928
			0.8	0.263	0.9940
			0.6	0.281	0.9953
			0.4	0.307	0.9966
$\frac{b'}{a'} = 0.75$	0.2178	0.6866	1.0	0.250	0.9752
			0.8	0.263	0.9786
			0.6	0.281	0.9823
			0.4	0.307	0.9865
Isosceles Triangular Duct $2\alpha' = 20°$	0.1693	0.6332	1.0	0.250	0.9465
			0.8	0.263	0.9529
			0.6	0.281	0.9599
			0.4	0.307	0.9682
$2\alpha' = 40°$	0.1840	0.6422	1.0	0.250	0.9589
			0.8	0.263	0.9593
			0.6	0.281	0.9658
			0.4	0.307	0.9732
$2\alpha' = 60°$	0.1875	0.6462	1.0	0.250	0.9555
			0.8	0.263	0.9613
			0.6	0.281	0.9674
			0.4	0.307	0.9746

in pipes of different cross-sectional shapes are the same. It must be noted that the dimensionless entrance length is non-dimensionalized by twice the hydraulic radius, which changes with pipe cross-sectional shape. Thus, though the dimensionless entrance lengths for turbulent flow in pipes of all types of shapes are almost identical, the actual entrance length at the same Reynolds number is different by a factor equal to the hydraulic radius. As an engineering estimate, for turbulent flow in any non-circular pipe, the hydrodynamic entrance length for power-law fluids can be estimated by using a conservative value of $\lambda_1 = 1.05$ in Equation 70.

Annular Pipes

Entry region flow of non-Newtonian fluids in annular pipes has been treated for the laminar case by Tan and Tiu [10] and Bhattacharyya and Tiu [11, 12]. However, again there is no literature on similar treatise for turbulent flow. The procedure of Shenoy and Mashelkar [19] for estimating turbulent entrance lengths for power-law fluids could, nevertheless, be used for getting engineering estimates of entrance lengths in annular pipes.

As noted earlier, the shear stresses at the inner and outer wall of the annuli are different and therefore, it would be natural to expect two simultaneously developing boundary layer thicknesses—one starting from the inner wall, namely, δ_1 and the other from the outer wall, namely, δ_o, It is now assumed that the velocity profiles given by Equations 35 and 43 are valid at the edge of the corresponding boundary layers as a first approximation. Then using similar arguments as those used by Shenoy and Mashelkar [19] as detailed earlier, the expressions for the entrance lengths can be written:

$$\frac{x_{eo}}{F_o D_o} = \left[\frac{\psi_1}{(1+\beta n)\alpha\psi^2}\right] Re_o^{\beta} \tag{73}$$

$$\frac{x_{ei}}{F_i D_i} = \left[\frac{\psi_1}{(1+\beta n)\alpha\psi^2}\right] Re_i^{\beta} \tag{74}$$

where x_{eo} and x_{ei} are the entrance lengths for the outer and inner region, D_o and D_i are the outer and inner pipe diameters, Re_o and Re_i are the Reynolds numbers based on outer and inner equivalent diameters as defined below and F_o and F_i are geometric factors as shown in the following:

$$Re_o = \frac{D_{eo}^n V^{2-n}\rho}{\gamma}, \qquad Re_i = \frac{D_{ei}^n V^{2-n}}{\gamma} \tag{75}$$

$$D_{eo} = 2r_o[1-\lambda^2], \qquad De_i = 2r_i\left[\frac{\lambda^2}{k^2} - 1\right] \tag{76}$$

$$F_o = \frac{(1-\lambda)}{(1+\lambda)^{\beta n}}, \qquad F_i = \frac{(1-\lambda^2)}{(\lambda+k)}\left[\frac{k(1-\lambda)}{(\lambda^2-k^2)}\right]^{\beta n} \tag{77}$$

The radius of maximum velocity is determined as discussed by Singh et al. [20] from the following:

$$\frac{\lambda - k}{1-\lambda} = k^{0.343} \tag{78}$$

This equation is general in nature as can be seen from its validity in the two limiting cases of the annular geometry, namely, a circular pipe ($\lambda = o$) and a parallel plate channel ($\lambda = 1$), irrespective of the type of the fluid and hence could be used for power-law fluids. Figure 10 shows a plot of x_{ei}/F_iD_i, x_{eo}/F_oD_o as functions of Reynolds number in the range of $10^4 \leq Re \leq 10^5$.

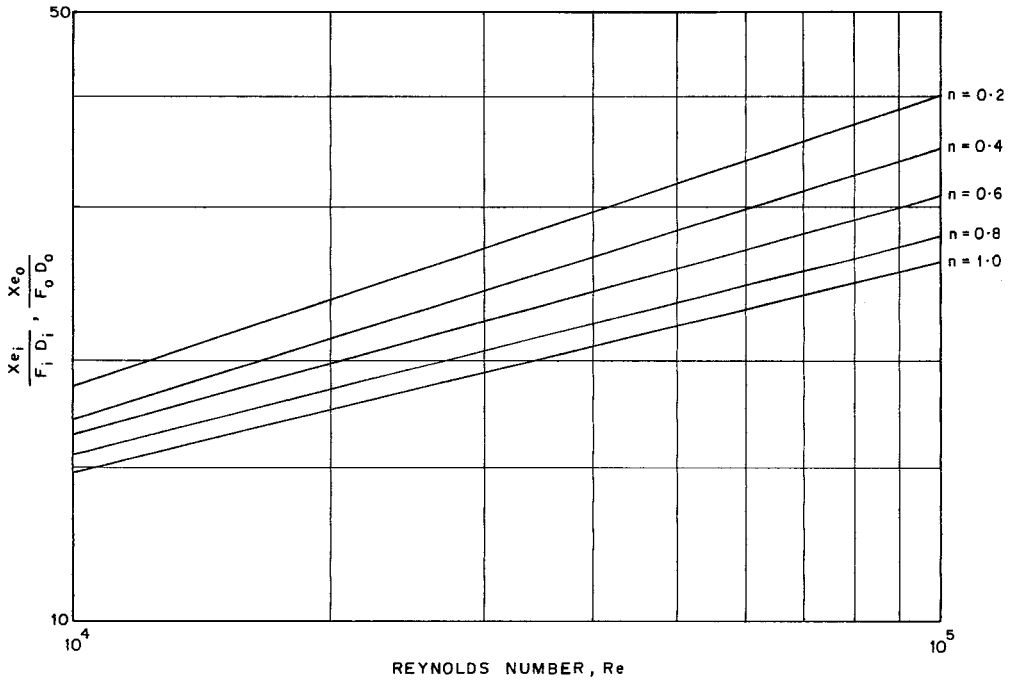

Figure 10. Entrance lengths for the inner and outer region of an annular pipe as a function of Reynolds number and pseudoplasticity index n.

CONCLUSION

This chapter deals with the nature of the time-averaged velocity profiles of turbulent pipe flow situations for inelastic non-Newtonian fluids in the absence of any anomalous effects, such as wall slip or drag reduction. The non-Newtonian characteristic of the fluid has been described by the power-law type Ostwald-de Waele fluid model. Several flow situations have been presented, such as those through circular and non-circular pipes as well as annular and curved pipes. In most cases, it is found that only a theoretical treatise has been done due to the dearth of experimental data in the literature. For smooth circular pipes alone experimental data is available and these have been reviewed by Edward and Smith [21]. The conclusions reached by them was that, if non-Newtonian velocity profiles were made dimensionless on a law of the wall basis with variables based on the apparent viscosity at the wall instead of Newtonian viscosity, the velocity profiles for non-Newtonian flows coincided with those for Newtonian flows.

Velocity profile measurements in turbulent flow with the use of heated or impact probes has had a variety of problems [22] due to the inherent flow disturbances caused by probes and their inaccurate sensitivity in non-Newtonian fluids. Presently, however, through the popular use of Laser-Doppler-Anemometry (LDA), it should be possible to determine velocity profiles in turbulent flow. In LDA measurement technique, the probes are photons, which are non-contact measuring elements. The frequency of the laser light is influenced by the moving particles of the fluid and the frequency shift is proportional to the particle velocity, thus making it an effective method for getting point to point data of the velocity field. One could thus expect that the theoretical expressions for power-law fluid velocity profiles in turbulent flow presented in this chapter would see experimental

verification in the near future. However, it must be noted that all the velocity profile expressions given in the foregoing sections are valid only for inelastic non-Newtonian fluids and would not provide correct predictions for viscoelastic fluids as the elasticity of such fluids plays a major role in altering the flow field.

NOTATION

a geometrical parameter for various cross-sectional shapes of ducts as tabulated in Tables 2 and 4

a' dimensions of the major axis for various cross-sectional shapes of ducts as given in Tables 2 and 4

$\bar{a}$ radius of curved pipe

A coefficient appearing in Equation 14 as a function of n

A_1 coefficient appearing in Equation 28 and defined by Equation 29

$\bar{A}_1$ coefficient appearing in Equation 36 and defined by Equation 41

b geometrical parameter for various cross-sectional shapes of ducts as tabulated in Tables 2 and 4

b' dimensions of the minor axis for various cross-sectional shapes of ducts as given in Tables 2 and 4

B coefficient appearing in Equation 14 as a function of n

$\bar{B}$ coefficient appearing in Equation 52

B_1 exponent appearing in Equation 28 and defined by Equation 30

$\bar{B}_1$ exponent appearing in Equation 36 and which is taken to be equal to B_1

B' exponent appearing in Equation 41 and defined by Equation 42

C Correction factor defined by Equations 9 and 15 for respective cases

D pipe diameter

D_1 coefficient appearing in Equation 44 and defined by Equation 47

D_i diameter of the inner pipe of an annulus

D_o diameter of the outer pipe of an annulus

D_{ei}, D_{eo} equivalent diameters defined by Equation 76

f friction factor

F_i, F_o geometric factors defined by Equation 77 for an annulus

I function appearing in Equation 8, values of which for varying Reynolds number and pseudoplasticity index are given in Table 1

k geometric factor defined by Equation 39 for an annulus

K consistency index for a power-law fluid as from Equation 2

L length of pipe

n pseudoplasticity index for a power-law fluid as from Equation 2

ΔP pressure drop across the length of the pipe

r radial position

r_H hydraulic radius appearing in Equation 32

r_i radius of the inner cylinder of an annulus

r_m radius of maximum velocity inside an annulus

r_o radius of the outer pipe of an annulus

R pipe radius

$\bar{R}$ the radius of curvature of a curved pipe as appearing in Equations 46 and 47

R^+ Reynolds number based on pipe radius and friction velocity

Re Reynolds number

Re_i, Re_o Reynolds number for power-law fluids as given in Equation 75 based on equivalent inner and outer diameters of an annulus

Re_ϵ roughness Reynolds number for power-law fluids as defined by Equations 53 and 54

Re_{gen} generalized Reynolds number for power-law fluids as defined by Equation 21

Re^*_{gen} generalized Reynolds number for power-law fluids for non-circular pipes as defined by Equation 32

T controlling term in the velocity profile for non-circular pipes as defined by Equation 34

T_1 controlling term in the velocity profile for rough pipes as defined by Equation 57

u time-averaged velocity at a point

u^* friction velocity defined as $\sqrt{\tau_w/\rho}$

u^+ dimensionless velocity defined as u/u*
u_i^* friction velocity for inner region of the annulus
u_o^* friction velocity for outer region of the annulus
u_i^+ dimensionless velocity for inner region of the annulus
u_o^+ dimensionless velocity for outer region of the annulus
u_m maximum velocity as defined by Equation 25
v angular velocity for a curved pipe as defined by Equation 44
v_m average axial velocity for the curved pipe appearing in Equations 47 and 48
V mean velocity of power-law fluid in a smooth circular pipe as defined by Equation 25
w axial velocity for a curved pipe as defined by Equation 45
w_1 coefficient appearing in Equation 45
w_c dimensionless axial velocity for a curved pipe as defined by Equations 48 and 51
x_e entrance length for smooth circular pipe as defined by Equation 69
x_{ei} entrance length for the inner region of an annulus and defined by Equation 74
x_{eo} entrance length for the outer region of an annulus and defined by Equation 73
$\bar{x}_c$ dimensionless entrance length for a circular pipe in Equation 72
$\bar{x}_{Nc}$ dimensionless entrance length for a non-circular pipe in Equation 72
y distance from the wall as shown in Figure 2
y_L laminar sublayer thickness as shown in Figure 2
y_T transition zone thickness as shown in Figure 2
y* dimensionless location parameter defined by y/R
y^+ distance based Reynolds number as defined by Equations 5 and 6
y_i^+ distance based Reynolds number for inner region of an annulus.
y_o^+ distance based Reynolds number for outer region of an annulus
y_2^+ transition zone thickness appearing in Equations 12 and 13

Greek Symbols

α coefficient appearing in Equation 23
α' half angle of an isosceles triangular duct appearing in Table 2
β exponent appearing in Equation 23
γ modified consistency index term defined by Equation 22
$\dot{\gamma}$ shear rate appearing in Equation 2
δ boundary layer thickness appearing in Equations 44 and 45
δ_c dimensionless boundary layer thickness as defined by Equation 46
ϵ average height of the roughness projections as shown in Figure 8.
η fluid viscosity
η_N Newtonian viscosity as shown in Figure 1
η_o zero-shear viscosity as shown in Figure 1
η_∞ infinite-shear viscosity as shown in Figure 1
λ dimensionless parameter for an annulus as defined by Equation 39
λ_1 dimensionless parameter for a non-circular pipe as defined by Equations 71 and 72
θ angular co-ordinate for a curved pipe as shown in Figure 4
ρ density of the fluid
σ_1 function of n defined by Equation 16
σ_2 function of n defined by Equation 17
τ shear stress apppearing in Equation 2
τ_w wall shear stress
τ_{wi} wall shear stress for inner region of an annulus as given by Equation 37
τ_{wo} wall shear stress for outer region of an annulus as given by Equation 38
ξ distance from the wall for curved pipe
ψ function of β and n as defined by Equation 26
ψ_1 function of β and n as defined by Equation 67

REFERENCES

1. Bird, R. B., Armstrong, R. C., and Hassager, O., *Dynamics of Polymeric Liquids: Volume I, Fluid Mechanics*, John Wiley and Sons, New York, 1977, pp. 205–212.
2. Langhaar, H. L., *Dimensional Analysis and Theory of Models*, John Wiley and Sons, New York, 1951.
3. Dodge, D. W., and Metzner, A. B., "Turbulent Flow of Non-Newtonian Systems," *AIChE J.*, Vol. 5. 1959, pp. 189–204.
4. Bogue, D. C., and Metzner, A. B., "Velocity Profiles in Turbulent Pipe Flow," *Ind. Eng. Chem. Fundam.*, Vol. 2, 1963, pp. 143–152.
5. Clapp, R. M., International Developments in Heat Transfer, Part III. 652–61; D-159; D–211-5, A.S.M.E., New York, 1961.
6. Shenoy, A. V., and Saini, D. R., "A New Velocity Profile Model for Turbulent Pipe-Flow of Power-Law Fluids," *Can. J. Chem. Eng.*, Vol. 60, 1982, pp. 694–696.
7. Skelland, A. H. P., *Non-Newtonian Flow and Heat Transfer*, John Wiley and Sons, New York, 1967, pp. 288–291.
8. Kozicki, W., Chou, C. H., and Tiu, C., "Non-Newtonian Flow in Ducts of Arbitrary Cross-Sectional Shape," *Chem. Eng. Sci.*, Vol. 21, 1966, pp. 665–679.
9. Salem, E., and Embaby, M. H., "Theoretical and Experimental Investigations of Non-Newtonian Fluid Flow Through Non-Circular Pipes," *Appl. Sci. Res.*, Vol. 33, 1977, pp. 119–139.
10. Tan, K. L., and Tiu, C., "Entry Flow Behavior of Viscoelastic Fluids in an Annulus," *J. Non-Newtonian Fluid Mechanics*, Vol. 3, 1977/1978, pp. 25–40.
11. Tan, K. L., and Tiu, C., "An Experimental Investigation of Upstream Flow Characteristics of Viscoelastic Fluids in an Annular Die Entry," *J. Non-Newtonian Fluid Mechanics*, Vol. 6, 1979, pp. 21–45.
12. Tan, P. K. L., and Tiu, C., "Velocity Profiles of Viscoelastic Fluids at the Inlet of an Annulus," *AIChE J.*, Vol. 26, No. 1, 1980, pp. 162–165.
13. Tiu, C., and Tan, K. L., "Boundary Layer Analysis of Viscoelastic Flow in Annuli," *Rheol. Acta*, Vol. 16, 1977, pp. 497–509.
14. Bhattacharyya, S., and Tiu, C., "Developing Pressure Profiles for Non-Newtonian Flow in an Annular Duct," *AIChE J.*, Vol. 20, No. 1, 1974, pp. 154–158.
15. Tiu, C., and Bhattacharyya, S., "Developing and Fully Developed Velocity Profiles for Inelastic Power-Law Fluids in an Annulus," *AIChE J.*, Vol. 20, No. 6, 1974, pp. 1140–1144.
16. Mashelkar, R. A., and Devarajan, G. V., "Secondary Flows of Non-Newtonian Fluids: Part III—Turbulent Flow of Visco-Inelastic Fluids in Coiled Tubes: A Theoretical Analysis and Experimental Verification," *Trans. Instn. Chem. Engrs.*, Vol. 55, 1977, pp. 29–37.
17. Torrance, B., McK., *South African Mechanical Engr.*, Vol. 13, 1963, p. 89.
18. Schlichting, H., *BoundaryKLayer Theory* , McGraw-Hill, New York, 1968.
19. Shenoy, A. V., and Mashelkar, R. A., "Engineering Estimate of Hydrodynamic Entrance Lengths in Non-Newtonian Turbulent Flow," *Ind. Eng. Chem. Process Des. Dev.*, Vol. 22, 1983, pp. 165–168.
20. Singh, R. P., Nigam, K. K., and Mishra, P., "Developing and Fully Developed Turbulent Flow in an Annular Duct," *J. Chem. Eng.* Japan, Vol. 13, 1980, pp. 349–352.
21. Edwards, M. F., and Smith, R., "The Turbulent Flow of Non-Newtonian Fluids in the Absence of Anomalous Wall Effects," *J. Non-Newtonian Fluid Mech.*, Vol. 7, 1980, pp. 77–90.
22. Seyer, F. A., and Metzner, A. B., "Turbulence in Viscoelastic Fluids," Sixth Symp. Naval Hydrodynamics, Sept. 28–Oct. 4, 1966, pp. 19–38.